Broadband tunable instantaneous frequency measurement system based on stimulated Brillouin scattering*

LIAO Weijie, ZHANG Jiahong, and CAI Qibin**

Faculty of Information Engineering and Automation, Kunming University of Science and Technology, Kunming 650500, China

(Received 13 October 2022; Revised 29 November 2022)

A broadband tunable instantaneous frequency measurement (IFM) system is designed based on the stimulated Brillouin scattering effect of the highly nonlinear fiber in which the carrier suppressed single sideband modulated signal of the Brillouin frequency shift acts as pump light. The amplitude comparison function (ACF) is constructed by the power radio of the two paths in the system. The frequency measurement range and measurement accuracy can be tuned by changing the frequency difference of the two phase modulation signals. The tunable frequency measurement ranges of 2—5 GHz, 2—10 GHz, 2—15 GHz, 2—20 GHz, and 2—24 GHz are realized, and the corresponding measurement accuracies are 3.64 dB/GHz, 2.17 dB/GHz, 1.87 dB/GHz, 1.22 dB/GHz, and 0.77 dB/GHz, respectively.

Document code: A **Article ID:** 1673-1905(2023)03-0174-5

DOI https://doi.org/10.1007/s11801-023-2174-2

Instantaneous frequency measurement (IFM) plays an important role in radar warning, electronic reconnaissance and signal intelligence. It is a signal processing method to quickly acquire the spectrum information of measurement microwave signals[1,2]. With the rapid development of information technology, due to the restriction of electronic bottleneck, the traditional electronic microwave signal frequency measurement technology has been gradually replaced by the microwave photonics based frequency measurement technology[3-5]. Among the existing photonics based IFM techniques, the stimulated Brillouin scattering (SBS) effect based IFM method has aroused extensive research due to the advantages of larger measurement range and smaller measurement error[6-9].

By using SBS to assign a tunable phase shift on the optical carrier of an intensity modulated signal, a reconfigurable IFM system with adjustable measurement range and resolution is designed[10]. It is switchable between a tunable measurement range of 0—2 GHz with a resolution of ±50 MHz and a fixed measurement range of 0—12 GHz with a resolution of ±250 MHz. An IFM system by monitoring the optical powers based on birefringence effects in the highly nonlinear fiber (HNLF) is proposed[11]. By adjusting the operational parameters of the optical pump signal, a complementary polarization domain interferometer (PDI) pair with tunable free spectral range (*FSR*) is established. A frequency measurement range of 2.5—30 GHz (except 16—17.5 GHz) is achieved with a measurement error of 0.5 GHz and a measurement accuracy within 2.5 dB/GHz. A photonic frequency measurement approach based on phase modulation is proposed and experimentally demonstrated[12]. A frequency measurement over a range of 1.6—24.6 GHz with measurement errors within ±0.3 GHz and a measurement accuracy of 2.9 dB/GHz is achieved. A photonic measurement method of microwave frequency by using phase modulators, tunable optical filters and a silicon microring resonator (MRR)[13] is proposed. By tuning the wavelengths of the laser diode, a tunable microwave photonic filter (MPF) with a measurement range of 10—19 GHz, a measurement resolution of 0.08 GHz and a measurement accuracy of 30 dB/GHz is achieved. Based on the tunable MPF, a reconfigurable IFM system is proposed. A non-sliced broadband optical source (BOS) is used to realize two tunable MPFs with equivalent infinite taps[14]. By simply adjusting two variable optical delay lines (VODLs), the frequency measurement ranges of 8—16.5 GHz and 11.5—20 GHz with a measurement accuracy less than 110 MHz can be realized. A high-precision IFM system with highly simple configuration exploiting SBS and an apodised fiber Bragg grating (AFBG) is proposed[15]. The blind spot in the measurement range can be eliminated by utilizing two single mode fibers (SMFs) with different Brillouin frequency shifts (BFSs). A measurement error of less than ±1 MHz within 10.68—20 GHz is achieved. In addition, many IFM systems based on the SBS are proposed[16-20], achieving larger measurement range and smaller measurement error. But the measurement ranges are not tunable

* This work has been supported by the National Science Foundation of China (No.62162034), and the General Program of Basic Research Program of Yunnan Province (No.202201AT070189).
** E-mail: zjh_mit@163.com

and their structures are not flexible enough.

In this paper, a broadband tunable IFM system is proposed based on dual-symmetric SBS effect of the HNLF, in which the carrier suppressed single sideband modulated signal of the Brillouin frequency shift acts as the pump light. The frequency measurement is realized by using the radio of two output powers to construct amplitude comparison function (ACF). Through adjusting the frequency difference between the two phase-modulation signals f_{s1} and f_{s2}, a broadband tunable IFM system is realized.

The basic structure of the broadband tunable IFM system based on the dual-symmetric SBS is shown in Fig.1. The light wave output from the tunable laser is divided into two paths by an optical coupler 1 (OC1). The upper branch optical carrier is split into two paths via optical coupler 2 (OC2) and modulated by two phase modulators. The spectra of the two phase-modulated signals are shown in Fig.2(a) and (b), respectively. Under small signal modulation, only the optical carrier and the first-order sidebands are considered, and the output optical field of the phase modulated signal can be expressed as

$$E(t)=J_0(m)\exp(\mathrm{j}2\pi f_c t)+J_1(m)\exp\left\{\mathrm{j}\left[2\pi(f_c+f_{s1,2})t+\frac{\pi}{2}\right]\right\}-J_1(m)\exp\left\{\mathrm{j}\left[2\pi(f_c-f_{s1,2})t-\frac{\pi}{2}\right]\right\},\quad(1)$$

where m is the phase modulation index, f_c is optical carrier frequency, f_{s1} and f_{s2} are the frequencies of the phase modulated signals, and $J_n(\cdot)$ represents the nth-order Bessel function of the first kind with n=0, ±1. In order to prevent the backward transmission of light in the optical path, the signal first passes through the optical isolator (ISO) and then enters the HNLF as the signal light. The lower branch optical carrier is modulated via the dual-parallel Mach-Zehnder modulator 1 (DPMZM1), which is driven by the Brillouin frequency shift f_b, and then the output of the DPMZM1 is modulated via the dual-parallel Mach-Zehnder modulator 2 (DPMZM2), which is driven by the unknown signal f_x to realize SSB-SC. The spectrum of the SSB-SC signal is shown in Fig.2(c). The SSB-SC signal output from the DPMZM2 is amplified by the semiconductor optical amplifier (SOA) and enters the HNLF by the optical coupler 3 (OC3) to act as the pump light. When the signal light interacts with the reverse-propagating pump light, the SBS effect occurrs and the amplitude of signal light is amplificated or attenuated, as shown in Fig.2(d) and (e). The balance of the phase modulated sidebands is broken and then converted into the intensity modulation.

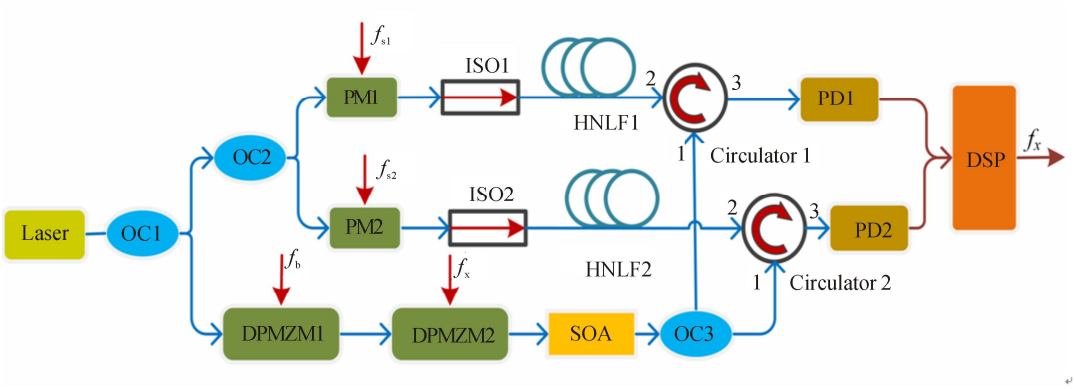

LD: laser diode; OC: optical coupler; PM: phase modulator; ISO: isolator; HNLF: high nonlinear optical fiber; DPMZM: dual-parallel Mach-Zehnder modulator; SOA: semiconductor optical amplifier; PD: photodetector

Fig.1 Schematic diagram of the broadband tunable IFM system

In the system, the first-order upper sideband is used and then the Brillouin gain and loss can be expressed as[21]

$$g(f)=\frac{g_0}{2}\frac{(\Delta\nu_B/2)^2}{f^2+(\Delta\nu_B/2)^2}+\mathrm{j}\frac{g_0}{4}\frac{(\Delta\nu_B/2)f}{f^2+(\Delta\nu_B/2)^2},\quad(2)$$

$$a(f)=-\frac{g_0}{2}\frac{(\Delta\nu_B/2)^2}{f^2+(\Delta\nu_B/2)^2}-\mathrm{j}\frac{g_0}{4}\frac{(\Delta\nu_B/2)f}{f^2+(\Delta\nu_B/2)^2},\quad(3)$$

where g_0 is the gain coefficient, $\Delta\nu_B$ is the Brillouin linewidth, and f is the frequency offset to center of the Brillouin linewidth of gain (for $g(f)$) or loss (for $a(f)$).

The optical field after the SBS effect can be given by

$$E(t)=\exp(\mathrm{j}2\pi f_c t)\{J_0(m)+J_1(m)\exp\{g[(f_p-f_B)-(f_c+f_{s1,2})]+a[(f_p+f_B)-(f_c+f_{s1,2})]+\mathrm{j}\left(2\pi f_{s1,2}t+\frac{\pi}{2}\right)\}-J_1(m)\exp\left[-\mathrm{j}\left(2\pi f_{s1,2}t+\frac{\pi}{2}\right)\right]\},\quad(4)$$

where f_p=f_c+f_b+f_x represents pump frequency, and f_x is the unknown frequency. Then Eq.(4) can be rewritten as

$$E(t)=\exp\left(\mathrm{j}2\pi f_{\mathrm{c}}t\right)\{J_0\left(m\right)+J_1\left(m\right)\exp[g\left(f_{\mathrm{x}}-f_{\mathrm{s1,2}}\right)+$$
$$a\left(f_{\mathrm{x}}+2f_{\mathrm{B}}-f_{\mathrm{s1,2}}\right)+\mathrm{j}\left(2\pi f_{\mathrm{s1,2}}t+\frac{\pi}{2}\right)]-$$
$$J_1\left(m\right)\exp\left[-\mathrm{j}\left(2\pi f_{\mathrm{s1,2}}t+\frac{\pi}{2}\right)\right]\}. \quad (5)$$

Ignoring the direct current (DC) and the second harmonic components, the output optical power is expressed as

$$p(f)=2J_0(m)J_1(m)*\{G(f)A(f)\cos[2\pi f_{\mathrm{s1,2}}t+\frac{\pi}{2}+$$
$$\varphi_{\mathrm{g}}(f)+\varphi_{\mathrm{a}}(f)]-\cos(2\pi f_{\mathrm{s1,2}}t+\frac{\pi}{2})\}. \quad (6)$$

According to Eqs.(2) and (3), $G(f)$=exp{Re[$g(f)$]}, $A(f)$=exp{Re[$a(f)$]}, $\varphi_{\mathrm{g}}(f)$=exp{Im[$g(f)$]}, and $\varphi_{\mathrm{a}}(f)$=exp{Im[$a(f)$]}. According to Eq.(6), the ACF is constructed by comparing the two output powers

$$ACF\left(f_{\mathrm{x}}\right)=\frac{P(f_{\mathrm{s1}})}{P(f_{\mathrm{s2}})}. \quad (7)$$

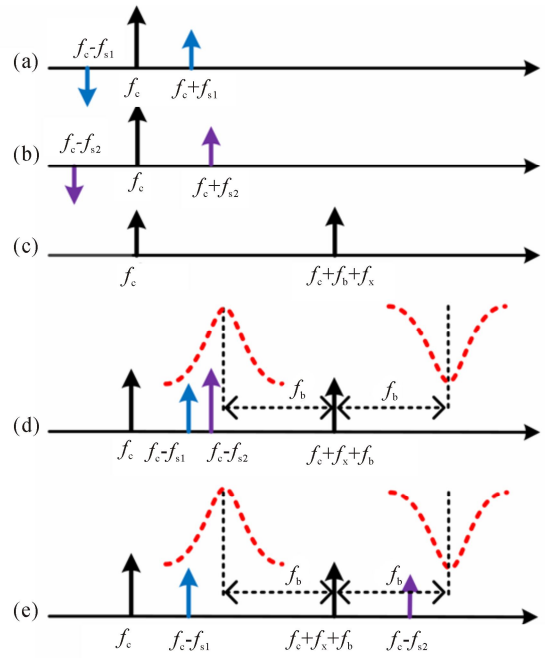

Fig.2 Spectrum processing diagram of SBS effect: (a) Phase modulation; (b) Phase modulation; (c) SSB-SC modulation; (d) SBS effect; (e) Spectrum after SBS effect

According to Eq.(7), when the phase modulation signals f_{s1}, f_{s2} and Brillouin frequency shift f_{b} are known, the ACF value corresponds to the unknown signal f_{x}. As a result, the approach for frequency measurement can be realized. Besides, when the frequency difference is changed, the ACF is changed and the measurement range is tuned accordingly. However, due to the different gain coefficient g_0, Brillouin frequency shift f_{b} and Brillouin linewidth $\Delta\nu_{\mathrm{B}}$ will both affect the ACF, and the influences of these parameters on the IFM system are analyzed.

Because the Brillouin frequency shift is $f_{\mathrm{b}}=2n_{\mathrm{f}}V_{\mathrm{a}}/\lambda_{\mathrm{p}}$ (n_{f} is the effective refractive index of the fiber, V_{a} is the speed of sound wave, and λ_{p} denotes the wavelength of the pump wave), the effect of λ_{p} on the ACF is analyzed, and the results are shown in Fig.3. From Fig.3, with λ_{p} of 1 500 nm, 1 530 nm, 1 550 nm, 1 570 nm, and 1 600 nm, the ACF slopes are 56.16 dB, 56.69 dB, 57.16 dB, 55.86 dB, and 56.04 dB, respectively, which correspond to the frequency measurement ranges of 2—23.99 GHz, 2—23.99 GHz, 2—24 GHz, 2.52—23.99 GHz and 4.57—23.99 GHz. When λ_{p} is 1 550 nm, the slope of the ACF is a maximum of 57.16 dB and the measurement range is also a maximum of 22 GHz. Therefore, λ_{p} is designed as 1 550 nm in the proposed IFM system.

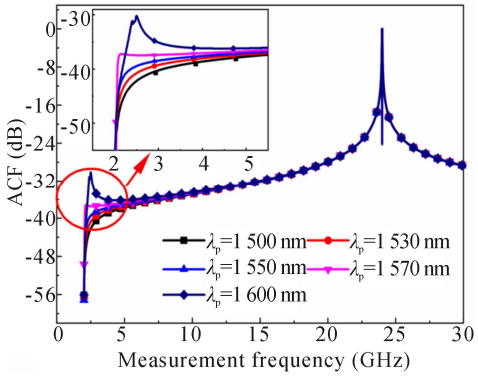

Fig.3 The ACF under different λ_{p}

From Eqs.(2) and (3), because the gain coefficient $g_0=g_{\mathrm{B}}I_{\mathrm{P}}L_{\mathrm{eff}}A_{\mathrm{eff}}$ (g_{B} is the line center gain, L_{eff} and A_{eff} are the effective fiber length and the effective mode area of HNLF, and I_{P} is the power of pump wave) affects the ACF, the influence of g_0 on the IFM is analyzed. The results are shown in Fig.4. From Fig.4, when g_0 is 1, 2, 3, 4, and 5, respectively, the ACF slope is 40.26 dB, 43.38 dB, 46.81 dB, 50.20 dB, and 53.55 dB, which correspond to the frequency measurement ranges of 2—24.02 GHz, 2—23.99 GHz, 2—23.99 GHz, 2—24.01 GHz and 2—24.02 GHz. Thus, as g_0 increases, the ACF slope increases by 13.29 dB, but the frequency measurement range change is small. Therefore, g_0 is designed as 5 in the IFM system.

In addition, different Brillouin linewidth $\Delta\nu_{\mathrm{B}}$ affects the ACF, and considering the general value of $\Delta\nu_{\mathrm{B}}$ is from 20 MHz to 100 MHz, Fig.5 shows the ACF under various $\Delta\nu_{\mathrm{B}}$. From Fig.5, when $\Delta\nu_{\mathrm{B}}$ is 20 MHz, 40 MHz, 60 MHz, 80 MHz, and 100 MHz, the slope of the ACF is 60.40 dB, 59.16 dB, 55.46 dB, 52.47 dB, and 49.97 dB, respectively, which correspond to the frequency measurement ranges of 2.01—23.99 GHz, 2—23.99 GHz, 2.01—23.99 GHz, 2.02—23.98 GHz and 2.02—23.98 GHz. It can be seen that $\Delta\nu_{\mathrm{B}}$ has little influence on the frequency measurement. Therefore, considering the ACF slope, $\Delta\nu_{\mathrm{B}}$ is designed as 20 MHz in the IFM system.

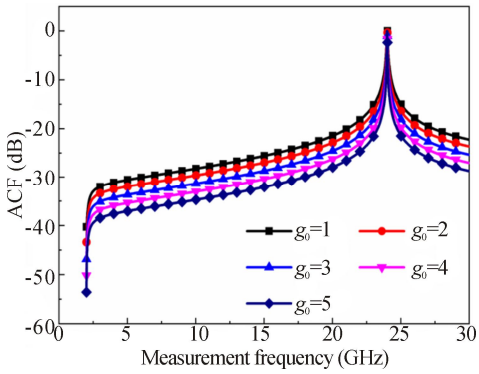

Fig.4 The ACF under different g_0

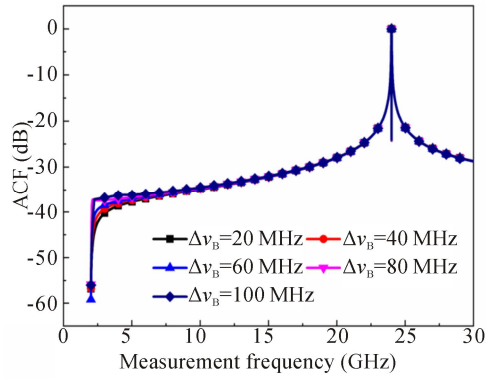

Fig.5 The ACF under different $\Delta\nu_B$

Based on the above analysis, parameters of the IFM system are designed as λ_p=1 550 nm, g_0=5, $\Delta\nu_B$=20 MHz. When f_{s2} is 2 GHz, adjusting f_{s1} to be 5 GHz, 10 GHz, 15 GHz, 20 GHz, and 24 GHz, respectively, as the input frequency f_x varies from 0 GHz to 30 GHz with step of 10 MHz, the measured ACF results are shown in Fig.6. From Fig.6, with f_{s1} of 5 GHz, 10 GHz, 15 GHz, 20 GHz, and 24 GHz, the ACF slopes are 53.72 dB, 61.72 dB, 64.73 dB, 64.76 dB, and 54.72 dB, which correspond to the frequency measurement ranges of 2—5 GHz, 2—10 GHz, 2—15 GHz, 2—20 GHz, and 2—24 GHz, and the measurement accuracies of 3.64 dB/GHz, 2.17 dB/GHz, 1.87 dB/GHz, 1.22 dB/GHz, and 0.77 dB/GHz, respectively. As a result, the measurement range can be tuned by adjusting the frequency difference of the phase modulated signal. However, the wider measurement range leads to lower accuracy.

The detailed comparison results are shown in Tab.1. From Tab.1, by adjusting the frequency f_{s1} from 5 GHz to 24 GHz, the measurement range can be tuned from 2—5 GHz to 2—24 GHz, and the corresponding ACF slope is changed from 53.72 dB to 54.72 dB, but the measurement accuracy is decreased from 3.64 dB/GHz to 0.77 dB/GHz. Therefore, a tradeoff between the frequency measurement range and accuracy should be considered in practical IFM systems.

In addition, the performance comparison of existing IFM systems has been shown in Tab.2. As can be seen from Tab.2, in Ref.[12], the wider measurement range has been achieved, but the range is not adjustable. In Ref.[13], the highest frequency measurement accuracy has been obtained, but the tunable range is smaller. In Ref.[14], the largest measurement range with lower accuracy and smaller tunable range has been obtained. In Ref.[15], a smaller tunable measurement range has been obtained. Therefore, the proposed IFM system has features of wider tunable range and flexible architecture compared to these existing IFM systems.

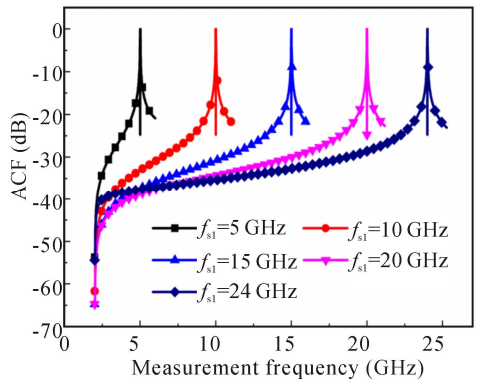

Fig.6 Measurement results

Tab.1 Measurement results

Frequency difference (GHz)	3	8	13	18	22
ACF slope (dB)	53.72	61.72	64.73	64.76	54.72
Measurement range (GHz)	2—5	2—10	2—15	2—20	2—24
Measurement accuracy (dB/GHz)	3.64	2.17	1.87	1.22	0.77

Tab.2 Performance comparison of existing IFM systems

Technology	Measurement range (GHz)	Tunable range (GHz)	Accuracy (dB/GHz)
PM + SMF[12]	1.6—24.6	0	2.9
MRR + MPFs[13]	10—19	9	30
MPFs + VODLs[14]	0—40	8.5	3.46
SBS + AFBG[15]	10.68—20	9.32	-
This work	2—24	22	3.64

In conclusion, a broadband tunable IFM system based on double-symmetric SBS effect is designed and analyzed. In order to construct the ACF, the carrier suppressed single sideband modulated signal of the Brillouin frequency shift and unknown frequency is used as the pump light in the two paths. By adjusting the frequency difference from 3 GHz, 8 GHz, 13 GHz, 18 GHz and 22 GHz, the frequency measurement ranges can be tuned

in 2—5 GHz, 2—10 GHz, 2—15 GHz, 2—20 GHz, and 2—24 GHz, which correspond to the measurement accuracies of 3.64 dB/GHz, 2.17 dB/GHz, 1.87 dB/GHz, 1.22 dB/GHz, and 0.77 dB/GHz, respectively. The results reveal that the proposed approach has a potential to be used in a broadband tunable IFM system.

Statements and Declarations

The authors declare that there are no conflicts of interest related to this article.

References

[1] CAPMANY J, MORA J, GASULLA I, et al. Microwave photonic signal processing[J]. Journal of lightwave technology, 2012, 31(4)：571-586.

[2] ZHANG H, PAN S. High resolution microwave frequency measurement using a dual-parallel Mach-Zehnder modulator[J]. IEEE microwave and wireless components letters, 2013, 23(11)：623-625.

[3] FENG D, XIE H, QIAN L, et al. Photonic approach for microwave frequency measurement with adjustable measurement range and resolution using birefringence effect in highly non-linear fiber[J]. Optics express, 2015, 23(13)：17613-17621.

[4] JIAO W, YOU K, SUN J. Multiple microwave frequency measurement with improved resolution based on stimulated Brillouin scattering and nonlinear fitting[J]. IEEE photonics journal, 2019, 11(1)：1-12.

[5] XU E, WANG Q, WANG F, et al. Instantaneous microwave frequency measurement based on hybrid microwave photonic filter[J]. Optoelectronics letters, 2014, 10(5)：374-377.

[6] JIAO W, CHENG M, WANG K, et al. Demonstration of photonic-assisted microwave frequency measurement using a notch filter on silicon chip[J]. Journal of lightwave technology, 2021, 39(21)：6786-6795.

[7] ZHENG S, GE S, ZHANG X, et al. High-resolution multiple microwave frequency measurement based on stimulated Brillouin scattering[J]. IEEE photonics technology letters, 2012, 24(13)：1115-1117.

[8] JING N, GU J, LIU W, et al. A multiple microwave frequency measurement based on stimulated Brillouin scattering in few-mode optical fiber[J]. Optical fiber technology, 2019, 53：102013.

[9] DONG R, JIANG Y, LUO H, et al. A coupled all-optical microwave oscillator with large tuning range based on SBS[J]. Optics communications, 2020, 477：126368.

[10] LI W, ZHU N H, WANG L X. Brillouin-assisted microwave frequency measurement with adjustable measurement range and resolution[J]. Optics letters, 2012, 37(2)：166-168.

[11] FENG D, XIE H, QIAN L, et al. Photonic approach for microwave frequency measurement with adjustable measurement range and resolution using birefringence effect in highly non-linear fiber[J]. Optics express, 2015, 23(13)：17613-17621.

[12] TU Z, WEN A, GAO Y, et al. A photonic technique for instantaneous microwave frequency measurement utilizing a phase modulator[J]. IEEE photonics technology letters, 2016, 28(24)：2795-2798.

[13] LIU L, XUE W, YUE J. Photonic approach for microwave frequency measurement using a silicon microring resonator[J]. IEEE photonics technology letters, 2018, 31(2)：153-156.

[14] SHI D, WEN J, ZHU S, et al. Instantaneous microwave frequency measurement based on non-sliced broadband optical source[J]. Optics communications, 2020, 458：124758.

[15] JIAO W, HUANG Q, HUANG C, et al. High-precision microwave frequency measurement based on stimulated Brillouin scattering with simple configuration[J]. Journal of lightwave technology, 2022.

[16] LONG X, ZOU W, CHEN J. Broadband instantaneous frequency measurement based on stimulated Brillouin scattering[J]. Optics express, 2017, 25(3)：2206-2214.

[17] JIAO W, YOU K, SUN J. Multiple microwave frequency measurement with improved resolution based on stimulated Brillouin scattering and nonlinear fitting[J]. IEEE photonics journal, 2019, 11(1)：1-12.

[18] HUANG L, LI Y, ZHAO S, et al. Functional flexible photonics-assisted frequency measurement based on combination of stimulated Brillouin scattering and a Mach-Zehnder interferometer[J]. Quantum electronics, 2021, 51(12)：1135.

[19] WANG D, ZHANG X, ZHAO X, et al. Photonic microwave frequency measurement with improved resolution based on bandwidth-reduced stimulated Brillouin scattering[J]. Optical fiber technology, 2022, 68：102803.

[20] GONG J, TAN Q, WANG D, et al. Bandwidth-reconfigurable microwave photonic filter based on stimulated Brillouin scattering effect spreading by vector modulation technology[J]. Microwave and optical technology letters, 2021, 63(12)：2985-2990.

[21] XIAO Y, GUO J, WU K, et al. Multiple microwave frequencies measurement based on stimulated Brillouin scattering with improved measurement range[J]. Optics express, 2013, 21(26)：31740-31750.